Supplement of SOIL, 12, 521–543, 2026
https://doi.org/10.5194/soil-12-521-2026-supplement

Supplement of

Formation of mineral-associated organic matter via rock weathering: an experimental test for the organo-metallic glue hypothesis

Kaori Matsuoka et al.

Correspondence to: Kaori Matsuoka (matsuoka.kaori811@naro.go.jp, kaori.matsuoka@hotmail.co.jp) and Rota Wagai (wagai@g.ecc.u-tokyo.ac.jp)

Supplementary tables and figures

Tables S1-S14

Table S1. Major elements (g kg^{-1}) in the initial granite, basaltic rocks, sand, and leaf compost materials used to prepare rock-OM mixtures for the incubation experiment.

	Si	Ti	Al	Fe	Mn	Mg	Ca	Na	K	P
Granite 38–75 µm	310	0.67	69	14	0.40	N.D.	8.4	33	34	N.D.
Basalt 38–75 µm	255	4.8	83	78	1.3	42	64	18	4.6	0.71
Basalt 20–38 µm	251	7.2	85	87	1.7	38	66	18	4.0	0.60
Sand 100–300 µm	394	0.43	17	2.3	0.066	N.D.	2.1	3.6	11	N.D.
Leaf compost	56	0.41	8.6	6.9	0.50	3.1	33	N.D.	3.7	1.1

Total elemental compositions were determined by XRF analysis (NEX CG, Rigaku Corporation, Tokyo, Japan).

$n = 1$

N.D. Not detected.

Table S2. Specific surface area ($m^2\ g^{-1}$) and extractable Al, Fe, and Si (mg g^{-1}) in the initial granite, basaltic rock, and sand used to prepare the rock-OM mixtures.

	Specific surface area
Granite 38–75 µm	0.73
Basalt 38–75 µm	2.9
Basalt 20–38 µm	3.5
Sand 100–300 µm	0.76

	Sodium pyrophosphate (PP)			Acid oxalate (OX)			Dithionite-citrate (DC)			Total		
	Al	Fe	Si	Al	Fe	Si	Al	Fe	Si	Al	Fe	Si
Granite 38–75 µm	N.D.	N.D.	N.D.	0.29 ± 0.01	0.77 ± 0.02	0.21 ± 0.01	0.35 ± 0.13	3.3 ± 1.1	1.7 ± 0.6	0.64 ± 0.13	4.0 ± 1.1	1.9 ± 0.7
Basalt 38–75 µm	0.17 ± 0.01	0.35 ± 0.03	0.59 ± 0.06	5.6 ± 0.1	32 ± 1	3.4 ± <0.1	0.82 ± 0.05	5.8 ± 0.8	10 ± 1	6.6 ± 0.1	38 ± 2	14 ± 1
Basalt 20–38 µm	0.22 ± 0.04	0.47 ± 0.07	0.76 ± 0.15	6.8 ± 0.8	40 ± 1	4.8 ± 0.7	0.77 ± 0.25	5.3 ± 1.6	7.8 ± 2.4	7.8 ± 0.9	46 ± 1	13 ± 3
Sand 100–300 µm	N.D.	N.D.	N.D.	0.027 ± 0.015	0.091 ± 0.027	N.D.	0.32 ± 0.24	2.9 ± 1.9	1.2 ± 1.1	0.35 ± 0.23	3.0 ± 1.9	1.2 ± 1.1

Al, Fe, and Si were extracted sequentially with sodium pyrophosphate, acid oxalate, and dithionite-citrate.

Value shows mean ± standard deviation (n = 3 for granite, basalts, and sand).

N.D. Not detected.

Table S3. Masses of the rock-OM mixtures before and after the 55-day incubation.

	Before (g)	After (g)
Granite 38–75 µm	20.00 g (crushed mineral) + 2.50 g (leaf compost) = 22.50	22.12 ± 0.03
Basalt 38–75 µm	same as above	22.44 ± 0.12
Basalt 20–38 µm	same as above	22.43 ± 0.18
Sand 100–300 µm	same as above	22.42 ± 0.12

Expressed on an air-dried basis.

Value shows mean ± standard deviation (n = 3).

Table S4. Gravimetric water content in the rock-OM mixtures at the start and end of wet-and-dry cycles during the 55-day incubation.

	Wet condition (%)	Dry condition (%)
Granite 38–75 μm	62 ± 1	~0
Basalt 38–75 μm	62 ± 1	~0
Basalt 20–38 μm	63 ± 1	~0
Sand 100–300 μm	52 ± 4	~0

The average water content of eight wet-and-dry cycles, expressed on an air-dried basis.

Value shows mean ± standard deviation (n = 3).

Table S5. Sample mass used for each analysis of the bulk rock-OM mixtures and meso-density fraction after the 55-day incubation.

	Bulk	Meso-density fraction (1.8–2.4 g cm^{-3})			
Fractionation / Measurement	All four treatments	Granite 38–75 μm	Basalt 38–75 μm	Basalt 20–38 μm	Sand 100–300 μm
Density fractionation	10.0 g				
Total C and N contents	0.5 g	≤0.05 g	≤0.35 g	≤0.3 g	≤0.02 g
C and N isotopic compositions	N.A.	N.A.	≤0.08 g	≤0.1 g	N.A.
Extractable Al, Fe, Si, Ca, and base cations	0.1 g	N.A.	0.1 g	0.1 g	N.A.
pH	0.4 g	N.A.	N.A.	N.A.	N.A.
Image analyses (SEM, STXM-NEXAFS)	<0.01 g	<0.01 g	<0.01 g	<0.01 g	N.A.
Microbial DNA extraction*	<0.4 g	0.01 g	0.1 g	0.1 g	N.A.
Total mass	<11.41	≤0.07	≤0.64	≤0.61	≤0.02

Expressed on an air-dried basis, except for microbial community analyses (on an oven-dried basis).

N.A. Not analyzed (due to the limited mass recovery of MF).

*A composite of three replications was used for the DNA extraction due to limited sample mass.

Table S6. Actual masses recovered in each density fraction from the rock-OM mixtures on Day 0 and Day 55. Mean ± standard deviation (n = 3).

Day 0 (total mass used: 4.0 g)*	Low-density fraction (< 1.8 g cm^{-3}) (g)	Meso-density fraction (1.8–2.4 g cm^{-3}) (g)	High-density fraction (> 2.4 g cm^{-3}) (g)	Total (g)
Granite 38–75 µm	N.A.	0.012 ± <0.001	4.0 ± <0.1	4.0 ± <0.1
Basalt 38–75 µm	N.A.	0.27 ± <0.01	3.6 ± <0.1	3.9 ± <0.1
Basalt 20–38 µm	N.A.	0.25 ± <0.01	3.7 ± <0.1	3.9 ± <0.1
Sand 100–300 µm	N.A.	0.0057 ± 0.0022	4.0 ± <0.1	4.0 ± <0.1
Day 55 (total mass used: 10.0 g)				
Granite 38–75 µm	0.91 ± 0.03	0.057 ± 0.001	8.9 ± 0.1	9.9 ± <0.1
Basalt 38–75 µm	0.93 ± 0.01	0.68 ± 0.04	7.9 ± <0.1	9.5 ± <0.1
Basalt 20–38 µm	1.1 ± <0.1	1.2 ± <0.1	7.2 ± <0.1	9.5 ± <0.1
Sand 100–300 µm	0.86 ± 0.02	0.017 ± <0.001	9.1 ± <0.1	10.0 ± <0.1

N.A. Not analyzed.

*The initial rocks (Day 0) were fractionated at the density of 2.4 g cm^{-3} only to isolate meso-density materials assuming that the initial leaf compost consists entirely of <1.8 g cm^{-3} low-density materials.

Table S7. List of mass, C content, and extractable metal data on per bulk sample and per fraction basis, presented as figures and tables in the main text and supplementary information.

Property	Timing	Per bulk or fraction	LF	MF	HF	Total
Mass	Initial material or mixture (Day 0)	/bulk	N.A.	Fig. 3a	N.A.	–
			---------- Table S3, S6 ----------			
	After incubation (Day 55)	/bulk	N.A.	Fig. 3a	N.A.	–
			---------- Fig. 2 ----------			
			---------- Table S3, S6 ----------			
C content (mg g^{-1})	Initial material	/bulk	---------- Table S8-2 ----------			
		/fraction	--------- Table S8-1 ---------			–
	After incubation	/bulk	---------- Table S9-2 ----------			
		/fraction	--------- Table S9-1 ---------			–
Extractable metals (mg g^{-1})	Initial material	/bulk	N.A.	Fig. 5	N.A.	Table S2
			---------- Table S10-2 ----------			
		/fraction	-------- Table S10-1 --------			–
	After incubation	/bulk	N.A.	Fig. 5	N.A.	–
			---------- Table S11 ----------			
		/fraction	---------- Table 2 ----------			–

N.A. Not analyzed.

Table S8-1. Concentrations of C and N (mg g^{-1} per fraction), and C:N ratio in each density fraction of the rock-OM mixtures on Day 0.

	Low-density fraction (< 1.8 g cm^{-3})						Meso plus high-density fraction* (> 1.8 g cm^{-3})	
	C		N		C:N ratio		C	
Granite 38–75 µm	408	± <1	10	± <1	41	± <1	0.18	± <0.01
Basalt 38–75 µm							0.33	± 0.02
Basalt 20–38 µm							0.24	± <0.01
Sand 100–300 µm							0.10	± 0.02

Value shows mean ± standard deviation (n = 3).

*C concentrations of the initial rock materials.

Table S8-2. Estimated distribution of C and N (mg g^{-1} bulk), and C:N ratio in each density fraction of the rock-OM mixtures on Day 0.

	Low-density fraction (< 1.8 g cm^{-3})						Meso-density fraction* (1.8–2.4 g cm^{-3})		High-density fraction* (> 2.4 g cm^{-3})		Sum of three fractions	
	C		N		C:N ratio		C		C		C	
Granite 38–75 µm	45	± <1	1.1	± <0.1	41	± <1	0.00048	± 0.00002	0.16	± <0.01	45	± <1
Basalt 38–75 µm							0.020	± <0.001	0.27	± <0.01	46	± <1
Basalt 20–38 µm							0.013	± <0.001	0.20	± <0.01	46	± <1
Sand 100–300 µm							0.00013	± 0.00005	0.089	± <0.001	45	± <1

Value shows mean ± standard deviation (n = 3).

*Carbon distribution between MF and HF was partitioned based on their mass distribution (Table S6) and C concentration (Table S8-1).

Table S9-1. Concentrations of C and N (mg g^{-1} per fraction) and C:N ratio in each density fraction from the rock-OM mixtures on Day 55.

	Low-density fraction (< 1.8 g cm^{-3})			Meso-density fraction (1.8–2.4 g cm^{-3})			High-density fraction (> 2.4 g cm^{-3})		
	C	N	C:N ratio	C	N	C:N ratio	C	N	C:N ratio
Granite 38–75 µm	427 ± <1	11 ± <1	40 ± <1	98 ± 3	5.2 ± <0.1	20 ± 1	0.54 ± <0.01	0.080 ± <0.001	5.1 ± 1.6
Basalt 38–75 µm	419 ± 5	11 ± <1	40 ± 1	13 ± <1	0.78 ± 0.07	17 ± 1	0.87 ± 0.03	0.13 ± 0.02	7.1 ± 0.9
Basalt 20–38 µm	378 ± 1	9.5 ± 0.1	40 ± <1	10 ± <1	0.71 ± 0.11	15 ± 2	1.0 ± <0.1	0.15 ± 0.02	6.9 ± 0.9
Sand 100–300 µm	431 ± 4	11 ± <1	40 ± 1	64 ± 6	4.4 ± <0.1	17 ± 2	0.29 ± 0.01	0.060 ± <0.001	3.6 ± 1.2

Value shows mean ± standard deviation (n = 3).

Table S9-2. Distribution of C and N (mg g^{-1} bulk) across the density fractions from the rock-OM mixtures on Day 55.

	Low-density fraction (< 1.8 g cm^{-3})		Meso-density fraction (1.8–2.4 g cm^{-3})		High-density fraction (> 2.4 g cm^{-3})		Sum of three fractions	
	C	N	C	N	C	N	C	N
Granite 38–75 µm	39 ± 1	0.99 ± 0.03	0.55 ± 0.03	0.028 ± 0.002	0.46 ± 0.02	0.12 ± 0.05	40 ± 1	1.1 ± <0.1
Basalt 38–75 µm	41 ± <1	1.0 ± <0.1	0.93 ± 0.04	0.056 ± 0.005	0.72 ± 0.02	0.10 ± 0.01	42 ± <1	1.2 ± <0.1
Basalt 20–38 µm	43 ± <1	1.1 ± <0.1	1.3 ± <0.1	0.090 ± 0.013	0.76 ± 0.01	0.11 ± 0.01	45 ± <1	1.3 ± <0.1
Sand 100–300 µm	37 ± <1	0.92 ± 0.03	0.10 ± 0.01	0.0063 ± 0.0012	0.25 ± 0.02	0.10 ± 0.04	37 ± <1	1.0 ± <0.1

Value shows mean ± standard deviation (n = 3).

Table S10-1. Theoretical* concentrations (mg g^{-1} per fraction) of extractable Al, Fe, and Si in each density fraction of the rock-OM mixtures on Day 0.

	Sodium pyrophosphate (PP)						Acid oxalate (OX)						Dithionite-citrate (DC)						Total					
	Al		Fe		Si		Al		Fe		Si		Al		Fe		Si		Al		Fe		Si	
Low-density fraction (< 1.8 g cm^{-3})																								
Leaf compost	0.075	± 0.009	0.10	± <0.01	4.4	± 0.1	1.5	± <0.1	1.5	± <0.1	0.91	± 0.05	0.38	± 0.02	1.0	± <0.1	2.2	± 0.1	1.9	± <0.1	2.6	± <0.1	7.5	± 0.2
Meso-density fraction (< 2.4 g cm^{-3})																								
Basalt 38–75 µm	0.28	± 0.01	0.84	± 0.04	1.2	± <0.1	12	± <1	44	± 1	6.3	± 0.2	2.3	± 0.1	15	± <1	11	± <1	14	± <1	59	± 1	19	± <1
Basalt 20–38 µm	0.31	± 0.01	1.0	± <0.1	1.2	± <0.1	16	± <1	59	± 1	8.3	± <0.1	2.4	± <0.1	15	± <1	10	± <1	19	± <1	75	± 1	20	± <1
High-density fraction (> 2.4 g cm^{-3})																								
Basalt 38–75 µm	0.20	± <0.01	0.35	± 0.02	0.71	± 0.05	5.4	± 0.2	30	± 1	3.7	± 0.1	0.42	± 0.05	3.5	± 0.2	10	± 1	6.0	± 0.1	34	± 1	15	± 1
Basalt 20–38 µm	0.19	± 0.01	0.40	± <0.01	0.92	± 0.33	4.5	± 0.1	31	± 1	3.2	± 0.1	0.41	± 0.05	4.7	± 0.3	10	± <1	5.1	± 0.1	36	± <1	14	± <1

Value shows mean ± standard deviation (n = 3 for basalts; n = 2 for leaf compost).

*The initial rocks (Day 0) were fractionated at the density of 2.4 g cm^{-3} to isolate the small amounts of meso-density materials assuming that the leaf compost consists fully of low-density materials.

Table S10-2. Theoretical* distribution of extractable Al, Fe, and Si (mg g^{-1} bulk) in each density fraction of the rock-OM mixtures on Day 0.

	Sodium pyrophosphate (PP)						Acid oxalate (OX)						Dithionite-citrate (DC)						Total					
	Al		Fe		Si		Al		Fe		Si		Al		Fe		Si		Al		Fe		Si	
Low-density fraction (< 1.8 g cm^{-3})																								
Leaf compost	0.0083	± 0.0010	0.011	± <0.001	0.49	± 0.02	0.16	± <0.01	0.17	± <0.01	0.10	± 0.01	0.042	± 0.002	0.11	± 0.01	0.24	± 0.01	0.21	± <0.01	0.29	± <0.01	0.83	± <0.01
Meso-density fraction (< 2.4 g cm^{-3})																								
Basalt 38–75 µm	0.017	± <0.001	0.051	± <0.001	0.071	± <0.001	0.72	± <0.01	2.6	± <0.1	0.38	± <0.01	0.14	± <0.01	0.91	± <0.01	0.67	± <0.01	0.88	± <0.01	3.6	± <0.1	1.1	± <0.1
Basalt 20–38 µm	0.017	± <0.001	0.055	± 0.001	0.069	± 0.001	0.89	± 0.02	3.3	± 0.1	0.46	± 0.01	0.13	± <0.01	0.82	± 0.01	0.56	± 0.01	1.0	± <0.1	4.2	± 0.1	1.1	± <0.1
High-density fraction (> 2.4 g cm^{-3})																								
Basalt 38–75 µm	0.16	± <0.01	0.29	± <0.01	0.59	± <0.01	4.4	± <0.1	25	± <1	3.0	± <0.1	0.35	± <0.01	2.9	± <0.1	8.4	± <0.1	4.9	± <0.1	28	± <1	12	± <1
Basalt 20–38 µm	0.16	± <0.01	0.33	± <0.01	0.77	± <0.01	3.7	± <0.1	26	± <1	2.7	± <0.1	0.34	± <0.01	3.9	± <0.1	8.3	± <0.1	4.2	± <0.1	30	± <1	12	± <1
Sum of three fractions																								
Basalt 38–75 µm	0.19	± <0.01	0.35	± <0.01	1.14	± <0.01	5.3	± <0.1	28	± <1	3.5	± <0.1	0.53	± <0.01	3.9	± <0.1	9.3	± <0.1	6.0	± <0.1	32	± <1	14	± <1
Basalt 20–38 µm	0.18	± <0.01	0.40	± <0.01	1.32	± <0.01	4.8	± <0.1	29	± <1	3.2	± <0.1	0.52	± <0.01	4.8	± <0.1	9.1	± <0.1	5.5	± <0.1	35	± <1	14	± <1

Al, Fe, and Si were extracted sequentially with sodium pyrophosphate, acid oxalate, and dithionite-citrate.

Value shows mean ± standard deviation (n = 3 for basalts; n = 2 for leaf compost).

*See Table S10-1 footnote.

Table S11. Distribution of extractable Al, Fe, and Si (mg g^{-1} bulk) in each density fraction of the rock-OM mixtures on Day 55.

	Sodium pyrophosphate (PP)			Acid oxalate (OX)			Dithionite-citrate (DC)			Total		
	Al	Fe	Si	Al	Fe	Si	Al	Fe	Si	Al	Fe	Si
Low-density fraction (< 1.8 g cm^{-3})												
Granite 38–75 µm	0.030 ± 0.003	0.023 ± 0.001	0.28 ± <0.01	0.094 ± 0.005	0.15 ± 0.01	0.047 ± 0.002	0.027 ± 0.003	0.14 ± 0.01	0.25 ± 0.02	0.15 ± 0.01	0.32 ± 0.02	0.57 ± 0.03
Basalt 38–75 µm	0.047 ± 0.001	0.051 ± 0.002	0.19 ± 0.01	0.13 ± 0.01	0.32 ± 0.01	0.065 ± 0.002	0.036 ± 0.001	0.20 ± <0.01	0.39 ± 0.01	0.22 ± 0.01	0.57 ± 0.01	0.64 ± 0.01
Basalt 20–38 µm	0.059 ± 0.002	0.080 ± 0.001	0.18 ± <0.01	0.23 ± 0.01	0.71 ± 0.02	0.13 ± <0.01	0.054 ± 0.001	0.37 ± 0.01	0.73 ± 0.01	0.34 ± 0.01	1.2 ± <0.1	1.0 ± <0.1
Sand 100–300 µm	0.033 ± 0.001	0.021 ± 0.001	0.26 ± 0.01	0.092 ± 0.005	0.14 ± 0.00	0.043 ± 0.001	0.022 ± 0.003	0.10 ± 0.01	0.21 ± 0.02	0.15 ± 0.01	0.26 ± 0.01	0.52 ± 0.03
Meso-density fraction (1.8–2.4 g cm^{-3})												
Granite 38–75 µm	N.A.	N.A.	N.A.	N.A.	N.A.	N.A.	N.A.	N.A.	N.A.	N.A.	N.A.	N.A.
Basalt 38–75 µm	0.031 ± 0.001	0.054 ± 0.002	0.12 ± 0.01	0.98 ± 0.26	3.7 ± 1.0	0.45 ± 0.12	0.19 ± 0.02	1.1 ± 0.1	0.68 ± 0.05	1.2 ± 0.3	4.9 ± 1.1	1.2 ± 0.2
Basalt 20–38 µm	0.057 ± 0.001	0.089 ± 0.005	0.22 ± 0.01	2.4 ± 0.1	9.5 ± 0.3	1.2 ± <0.1	0.31 ± <0.01	1.8 ± <0.1	1.2 ± <0.1	2.7 ± 0.1	11 ± <1	2.6 ± 0.1
Sand 100–300 µm	N.A.	N.A.	N.A.	N.A.	N.A.	N.A.	N.A.	N.A.	N.A.	N.A.	N.A.	N.A.
High-density fraction (> 2.4 g cm^{-3})												
Granite 38–75 µm	0.0 ± <0.1	0.0093 ± 0.0050	0.0 ± <0.1	0.11 ± 0.02	0.62 ± 0.03	0.12 ± 0.02	0.16 ± 0.01	1.7 ± <0.1	0.65 ± 0.02	0.27 ± 0.03	2.3 ± 0.1	0.78 ± 0.04
Basalt 38–75 µm	0.059 ± 0.009	0.19 ± 0.01	0.30 ± 0.02	3.1 ± 0.1	21 ± 1	1.9 ± 0.1	0.59 ± 0.03	4.0 ± 0.2	7.3 ± 0.2	3.7 ± 0.1	25 ± 1	9.5 ± 0.2
Basalt 20–38 µm	0.11 ± <0.01	0.21 ± <0.01	0.43 ± 0.01	3.5 ± 0.1	25 ± <1	2.4 ± <0.1	0.45 ± 0.04	3.7 ± 0.5	6.9 ± 0.1	4.1 ± 0.1	29 ± 1	9.7 ± <0.1
Sand 100–300 µm	0.0 ± <0.1	0.0 ± <0.1	0.0 ± <0.1	0.014 ± 0.008	0.13 ± 0.09	0.0 ± <0.1	0.080 ± 0.013	1.2 ± 0.2	0.073 ± 0.019	0.094 ± 0.011	1.3 ± 0.3	0.073 ± 0.019
Sum of three fractions												
Granite 38–75 µm	N.A.	N.A.	N.A.	N.A.	N.A.	N.A.	N.A.	N.A.	N.A.	N.A.	N.A.	N.A.
Basalt 38–75 µm	0.14 ± 0.01	0.30 ± 0.01	0.60 ± 0.03	4.2 ± 0.3	25 ± 1	2.4 ± 0.1	0.82 ± 0.02	5.3 ± 0.1	8.4 ± 0.2	5.2 ± 0.3	31 ± 1	11 ± <1
Basalt 20–38 µm	0.23 ± <0.01	0.38 ± <0.01	0.83 ± 0.01	6.1 ± 0.1	36 ± 1	3.7 ± 0.1	0.81 ± 0.04	5.9 ± 0.5	8.8 ± <0.1	7.2 ± 0.1	42 ± 1	13 ± <1
Sand 100–300 µm	N.A.	N.A.	N.A.	N.A.	N.A.	N.A.	N.A.	N.A.	N.A.	N.A.	N.A.	N.A.

Al, Fe, and Si were extracted sequentially with sodium pyrophosphate, acid oxalate, and dithionite-citrate.

Value shows mean ± standard deviation (n = 3).

N.A. Not analyzed due to the limited mass recovery of the meso-density fraction.

Table S12. Molar ratios of total C to sequentially extracted metals in meso-density fraction for the two basalt treatments after the 55-day incubation.

	Extraction reagent	Meso-density fraction (1.8–2.4 g cm^{-3})	
		C:Al	C:Fe
Basalt 38–75 μm	PP + OX	2.3 ± 0.9	1.3 ± 0.5
	PP + OX + DC	1.9 ± 0.7	1.0 ± 0.3
Basalt 20–38 μm	PP + OX	1.2 ± <0.1	0.64 ± 0.02
	PP + OX + DC	1.1 ± <0.1	0.54 ± 0.01

Al and Fe were extracted sequentially with sodium pyrophosphate (PP), acid oxalate (OX), and dithionite-citrate (DC).

Value shows mean ± standard deviation (n = 3).

Table S13. Cell number and alpha diversity index of the bacterial community in the meso-density fraction (1.8–2.4 g cm^{-3}; n = 1) for granite, coarse basalt, and fine basalt treatments and bulk for all four treatments (n = 3) on Day 55 compared to bulk in the initial leaf compost (n = 3).

			16S rRNA copy number (copies g^{-1} dry soil)		Chao1		Shannon		InvSimpson	
Granite 38–75 µm	Meso-density fraction	Day 55	1.51E+09		1833		5.3		23	
	Bulk	Day 55	4.25E+08	± 7.89E+07	1923	± 179	6.0	± 0.1	154	± 17
Basalt 38–75 µm	Meso-density fraction	Day 55	3.85E+08		1873		5.7		56	
	Bulk	Day 55	3.70E+08	± 1.04E+08	1906	± 79	5.8	± 0.2	91	± 39
Basalt 20–38 µm	Meso-density fraction	Day 55	5.47E+08		1574		5.6		77	
	Bulk	Day 55	3.84E+08	± 3.97E+07	1750	± 76	5.7	± 0.1	103	± 23
Sand 100–300 µm	Bulk	Day 55	6.20E+08	± 1.21E+08	1788	± 115	5.7	± 0.2	122	± 27
Leaf compost	Bulk	Day 0	9.49E+08	± 2.39E+08	1849	± 52	6.1	± 0.0	170	± 10

Value shows mean ± standard deviation (n = 3 for bulk samples).

Table S14. Mantel test showing the correlations between the bacterial composition and the mineral properties in the meso-density fraction for granite, coarse basalt, and fine basalt treatments on Day 55 (1.8–2.4 g cm^{-3}; n = 1), the bulk for all four treatments on Day 55 (n = 3), and the bulk for the initial leaf compost (n = 2).

Factor	R^2	P value
TC	**0.86**	0.001
TN	**0.86**	0.002
pH(KCl)	**0.82**	0.001
pH(H_2O)	**0.80**	0.001
Fe_{pp}	**0.30**	0.013
Al_{pp}	**0.22**	0.04
Fe_{ox}	0.22	0.068
Al_{ox}	0.14	0.286

Significant mantel coefficient is shown in bold.

Al and Fe were extracted sequentially with sodium pyrophosphate (PP), acid oxalate (OX), and dithionite-citrate.

Figures S1-S4

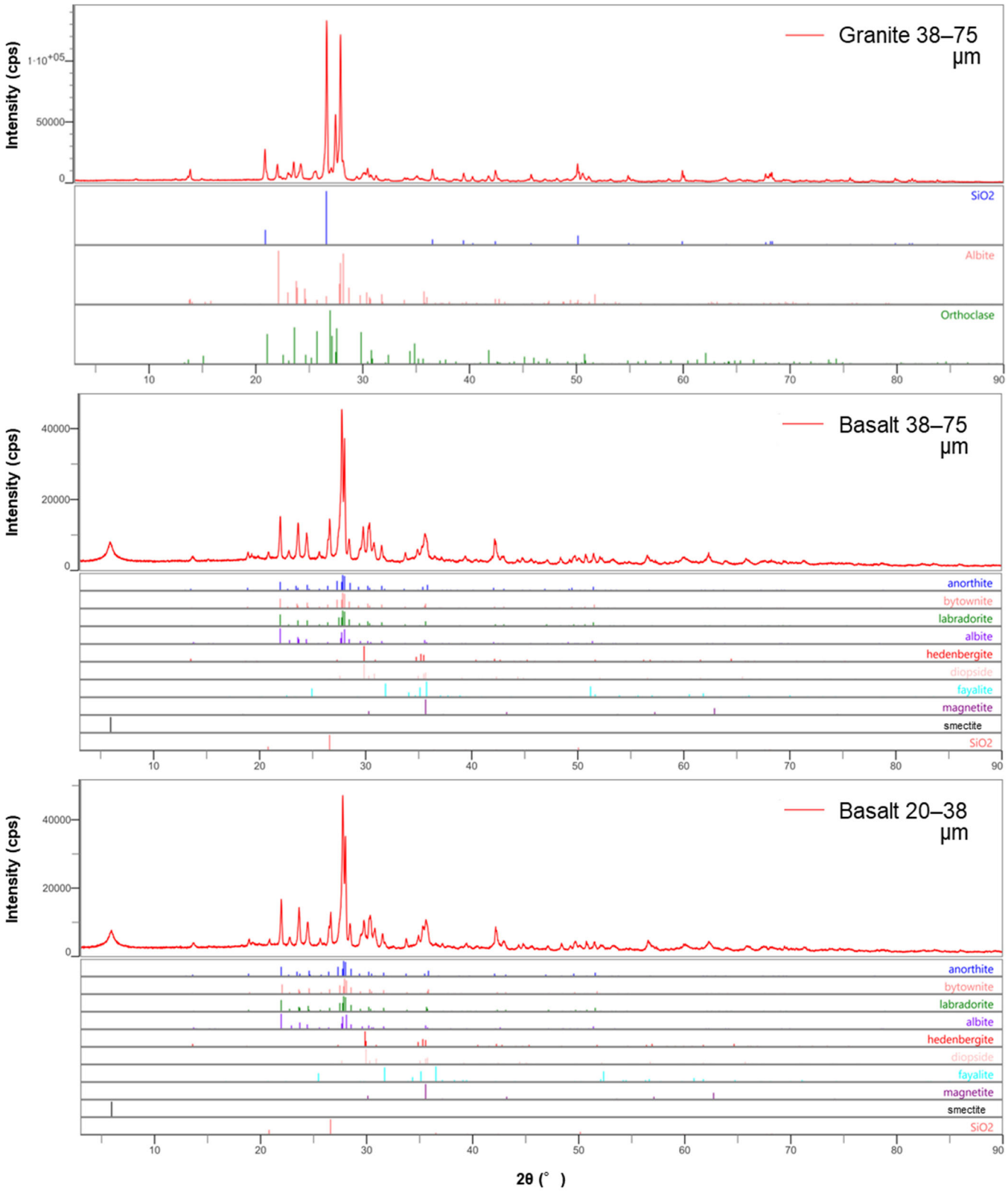

Figure S1. Mineralogical composition of the crushed rocks (granite, coarse basalt, and fine basalt) used in this experiment.

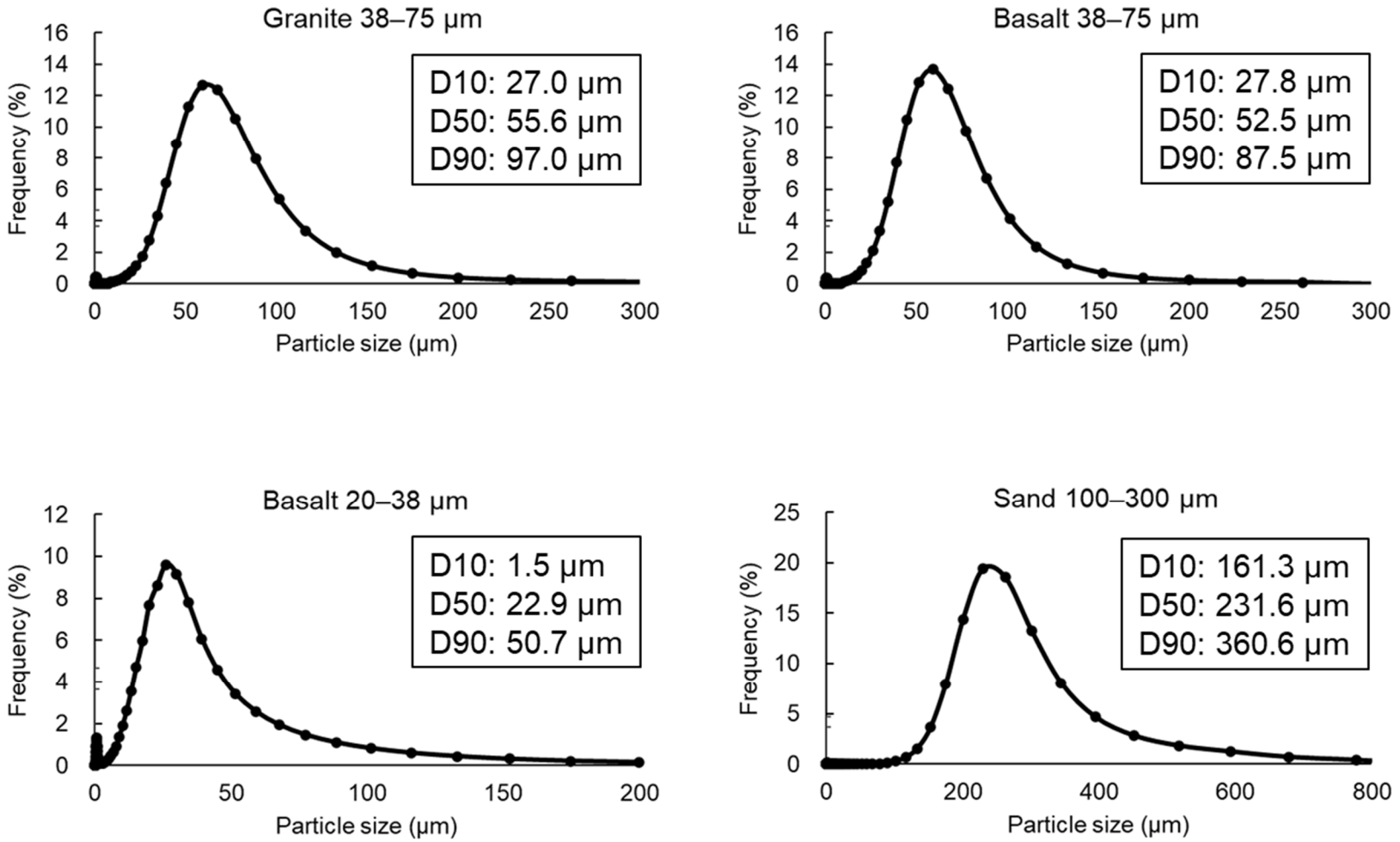

Figure S2. Particle size distribution of the crushed rocks (granite and basalt) and sand used in this experiment.

The granite (target size: 38–75 µm) had the mean weight diameter (MWD) of 63.9 µm and the cumulative percentile values (the grain size at which 50% of the grains are coarser, D50) of 55.6 µm (Fig. S1). The coarse basalt (38–75 µm) had a MWD of 59.8 µm and D50 of 52.5 µm. The fine basalt (20–38 µm) had a MWD of 28.8 µm and D50 of 22.9 µm. The sand (100–300 µm) had a MWD of 267.3 µm and D50 of 231.6 µm.

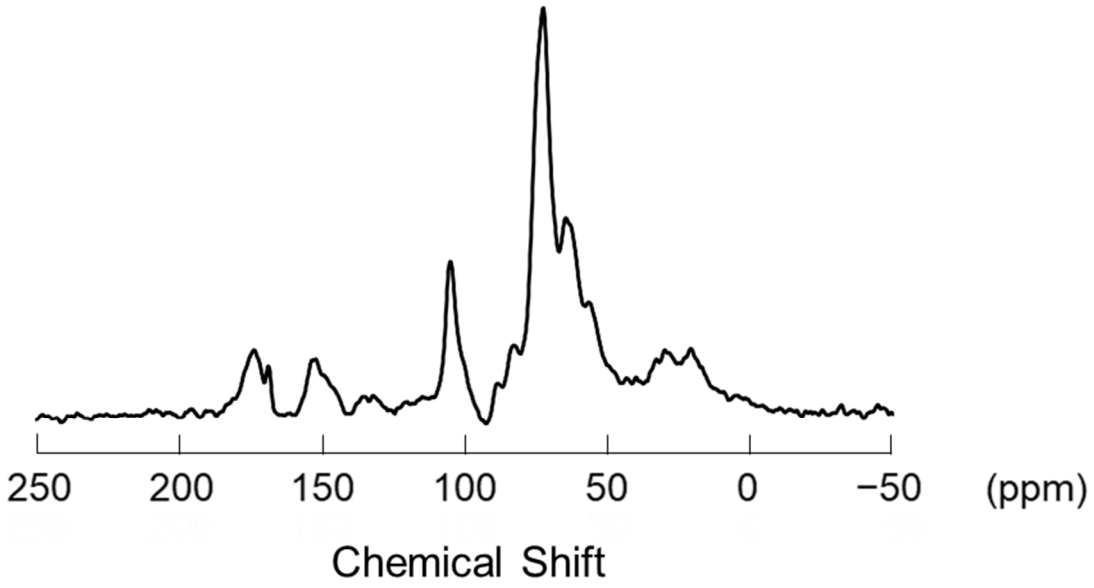

C type	(%)
Carbonyl-C	7.7
Aromatic-C	9.6
O-alkyl-C	63
Alkyl-C	19

Figure S3. Solid-state MS ^{13}C NMR spectrum and the proportion contributed by each C type to the total signal intensity in leaf compost used as a source of OM in this experiment.

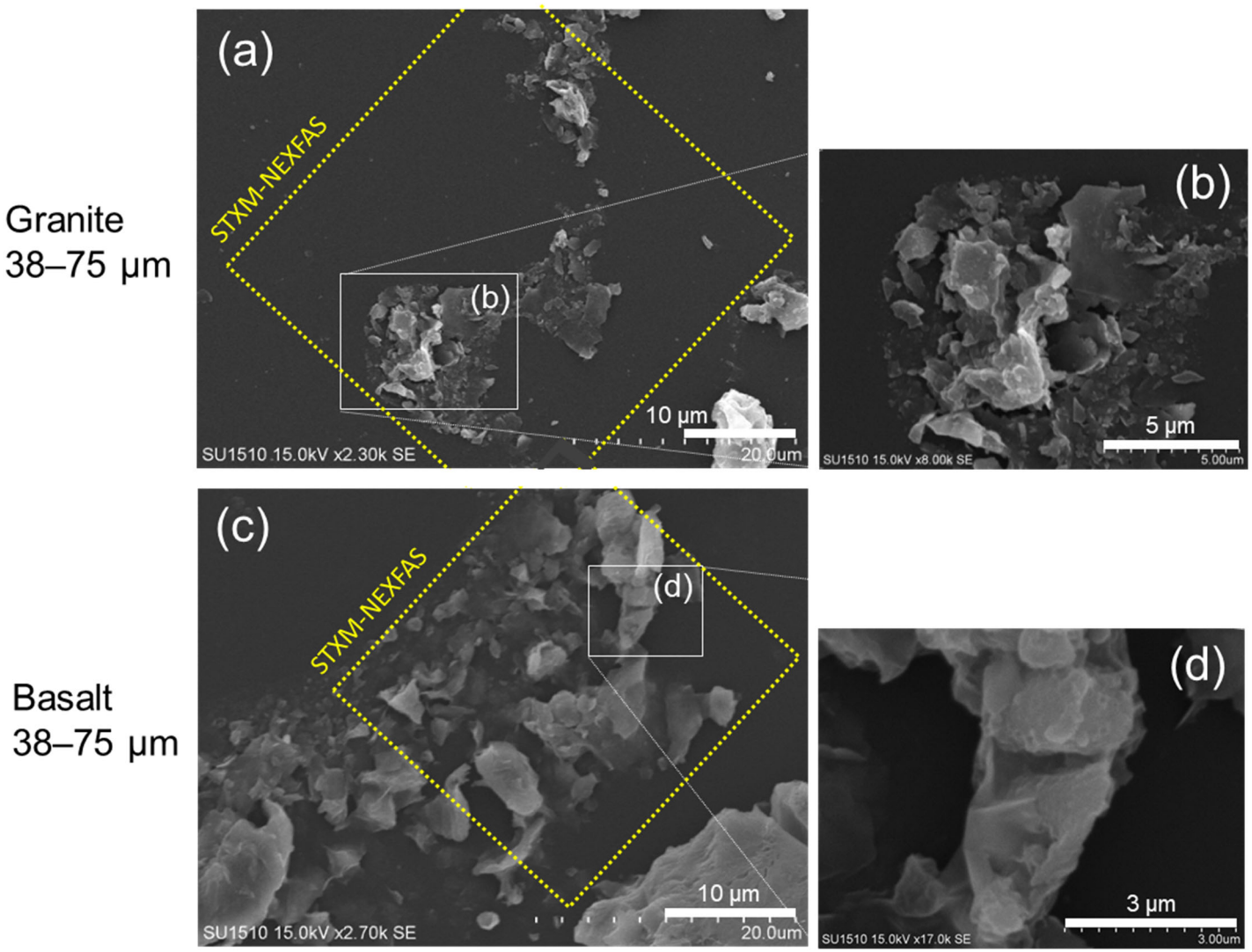

Figure S4. SEM images of dispersed particles from the meso-density fractions prepared for STXM-NEXAFS. Granite sample (a) and (b), and coarse basalt sample (c) and (d) after the incubation. The yellow dotted box in (a) and (c) represents the ROI used for STXM-NEXAFS analysis shown in Fig. 7 (A) and Fig. 7 (B), respectively. ROI (b) and (d) correspond to the higher resolution images used for STXM C optical density shown in Fig. 7 (a) and Fig. 7 (b), respectively.